

Molecular structure, vibrational, photophysical and nonlinear optical properties of L-threoninium picrate: A first-principles study

S. AlFaify^{a}, Mohd. Shkir^{a*}, M. Arora^b, Ahmad Irfan^{c,d}, H. Algarni^a, Haider Abbas^e, Shabbir Muhammad^a, Abdullah G. Al-Sehemi^{c,d}*

^a*Department of Physics, Faculty of Science, King Khalid University, P.O. Box. 9004 Abha 61413, Saudi Arabia*

^b*CSIR- National Physical Laboratory, Dr. K.S. Krishnan Road, New Delhi 110012, India*

^c*Department of Chemistry, Faculty of Science, King Khalid University, Abha 61413, P.O. Box 9004, Saudi Arabia*

^d*Research Center for Advanced Materials Science, King Khalid University, Abha 61413, P.O. Box 9004, Saudi Arabia*

^e*Department of Physics, Manav Rachna College of Engineering, Faridabad, Haryana 121001, India*

Corresponding author*

Dr. Mohd. Shkir

E-mail: shkirphysics@gmail.com, shkirphysics@kku.edu.sa,

Contact: +966 530683673, Fax: + 966 72418319

Abstract

In this work, different computational methods such as HF, B3LYP, range separated functionals (CAM-B3LYP and LC-BLYP) with 6-31G* basis set were applied to investigate the electronic, spectroscopic and nonlinear optical properties of L-threoninium picrate (LTHP) molecule for the first time. The calculated values of IR and Raman vibrational frequencies were found to be in a good agreement with the experimental results. Time dependent density functional theory has been applied to calculate the electronic and photophysical properties such as excitation energy, dipole moment and frontier molecular orbital (FMO) energies of LTHP molecule. The excitation energy value calculated by CAM-B3LYP is found to be at 351 nm which is in close agreement with the experimental values. The total/partial DOS (T/PDOS) was determined using GGA/BLYP. The total dipole moment (μ_{tot}), static total and anisotropy of polarizability (α_{tot} , $\Delta\alpha$) and static first hyperpolarizability (β_0 , β_{tot}) values were calculated and compared with the reference compound. The μ_{tot} and β_{tot} are found to be 3 and 51 time higher than urea molecule respectively. The FMOs, molecular electrostatic potential (MEP), global reactivity descriptors were also calculated and discussed. All these results suggest that the L-threoninium picrate would be a good candidate for optoelectronic device applications.

Keywords: IR and Raman spectroscopy, optical materials; optical properties; nonlinear optical material; DFT

1. Introduction

In recent years, the advancement in organic nonlinear optical (NLO) materials has increased enormously because of their impending applications in optoelectronic, electro-optic, photonic, semiconductors, ferroelectric and superconductors devices [1-4]. On the supramolecular level to demonstrate high second harmonic generation (SHG) output, the material should have the

structure of noncentrosymmetry, very strong intermolecular interactions and good phase-matching capability. On other hand the molecular scale, the amount of charge transfer is assumed to dominate the SHG output [5-7]. The materials which can transform the various parameters of optical beams such as frequency, phase, amplitude and polarization etc. are very important for NLO activity. The variety of materials including organic, inorganic, semiorganic, organometallic and polymeric have been studied for NLO applications. The organic materials receive the maximum attention because they are found to exhibit very high NLO response over a wide frequency range due to the presence of active π bonds. In addition to the above properties, these materials have large structural diversity, inherent synthetic flexibility, large optical damage threshold for laser power, low frequency dispersion, ultrafast response, photo stability, large first hyperpolarizability (β) and permit to modify the chemical structures and properties to achieve the desired NLO properties [8-10].

Picric acid acts as an electron acceptor and having very good tendency to synthesize the stable picrate complexes with a variety of organic compounds through strong hydrogen bonding or π interaction such as glycine, L-asparagine, 2-aminopyridine, 8-Hydroxyquinoline, L-proline and L-leucine etc. Their single crystals were also grown and studied previously [11-15]. These picrate compounds are found to show very large NLO response as well. Recently, a picrate compound named L-threoninium picrate (LTHP) has been synthesized by Natrajan et al. [16] and its crystal growth, structural, infrared, optical, and second harmonic generation efficiency (SHG) properties [SHG efficiency of LTHP was found to be 43 times that of standard potassium dihydrogen phosphate (KDP) crystals have been reported experimentally [16].

The quantum chemical approaches such as Hartree-Fock (HF) and density functional theory (DFT) which are cost effective general methods for analyzing almost all important properties

very accurately [17, 18]. The main advantages of HF and DFT are to determine and reproduce the reasonable and accurately molecular geometries and vibrational frequencies. Moreover, the range separated functionals such as CAM-B3LYP and LC-B3LYP are efficient to calculate the electronic and NLO properties which are much superior to the conventional methods [19-25].

The current available literature on the titled compound shows that there is no report on its theoretical studies so far. Due to excellent NLO response and other properties in the titled compound, its theoretical investigations seem to be necessary and justified to get deep insight of it for future device applications. Hence, in the current work our main aim is to report the various needful properties such as molecular geometry, electronic, infrared, vibrational, NLO and optical properties of recently developed compound L-threoninium picrate (LTHP) have been investigated using various computational methods. The calculated results were explained and compared with the experimental wherever available.

2. Computational details

The optimization of ground state molecular geometry [26-28] and vibrational frequency calculations for LTHP molecule have been performed at HF, B3LYP and CAM-B3LYP with 6-31G* basis set. Further, the electro-optical properties such as excitation energies, dipole moment and NLO properties of LTHP molecule have been calculated. HF and B3LYP methods were chosen because they are better methods for computation of molecular structures, IR spectra and Raman spectra. The time dependent density functional theory (TDDFT) using B3LYP and range separated functionals (CAM-B3LYP and LC-BLYP) has been applied to calculate the optical properties [20-22]. All the theoretical calculations on LTHP molecule have been performed with Gaussian G09 package software with the default convergence criteria, without any constraint on the geometry. To analyze all stationary points as minima for Infra-red (IR) and vibrational

(Raman) frequency calculations at DFT levels the optimized structural parameters were used. By taking the second derivative of energy the infrared and Raman spectra of LTHP were attained and computed analytically [29, 30].

Various other important parameters such as FMOs, dipole moment, polarizability, first hyperpolarizability and optical properties of LTHP were calculated. Finite Field (FF) method was applied to calculate the static first hyperpolarizability (β_{tot}) and its tensor components for the titled compound. The FF method was mostly applied to study the NLO properties because it can be used in concert with the electronic structure method to work out β values. Recently, the calculated β_{tot} by this method is found to be legitimate with experimental structure property relationship. In this method, a molecule is subjected to a static electric field (F) then the energy (E) is expressed by the following equation:

$$E = E^{(0)} - \mu_1 F_1 - \frac{1}{2} \alpha_{ij} F_i F_j - \frac{1}{6} \beta_{ijk} F_i F_j F_k - \frac{1}{24} \gamma_{ijkl} F_i F_j F_k F_l - \dots$$

where all the symbols are having their usual meanings and by differentiating this equation with respect to F the values of μ , α , β , and γ can be acquired.

3. Results and discussion

3.1. Molecular geometry

The optimized ground state molecular geometry of LTHP molecule was obtained by HF, B3LYP, and range separated functionals (CAM-B3LYP and LC-BLYP) with 6-31G* basis set. The geometry optimized by B3LYP and CAM-B3LYP using 6-31G* basis set along with numbering scheme has been figured out in Fig. 1 (a) and (b). The comparative important geometrical parameters such as bond lengths and bond angles are presented in Table 1 and found in close agreement with experimentally calculated values [16]. The hydrogen bond in LTHP molecule is shown by dotted lines [Fig. 1]. Two strong hydrogen bonds were observed between

picric acid and L-threonine molecules. The one hydrogen bond between H(11) and O(29) atom i.e., N(10)–H(11)---O(29) with bond length 1.561 Å and the second hydrogen bond between O(35) and H(36) i.e., O(15)–H(36)---O(35) with bond length 1.764 Å. While these bond lengths calculated by CAM-B3LYP [Fig. 1(b)] were found to be 1.534 and 1.768 Å, respectively. These bond length values show that the hydrogen bond is very strong between L-threonine and picric acid. An intra-molecular hydrogen bond between the amine N atom and the nearby oxygen atom, viz., N10–H12---O16, N10–H13---O14 and C2–H3---O16 were also observed with bond lengths 2.058, 2.665 and 2.643 Å, while these bond lengths calculated by CAM-B3LYP [Fig 1(b)] are found to be 2.047, 2.597 and 2.632 Å, respectively. The calculated bond lengths are very close to the experimental values [16].

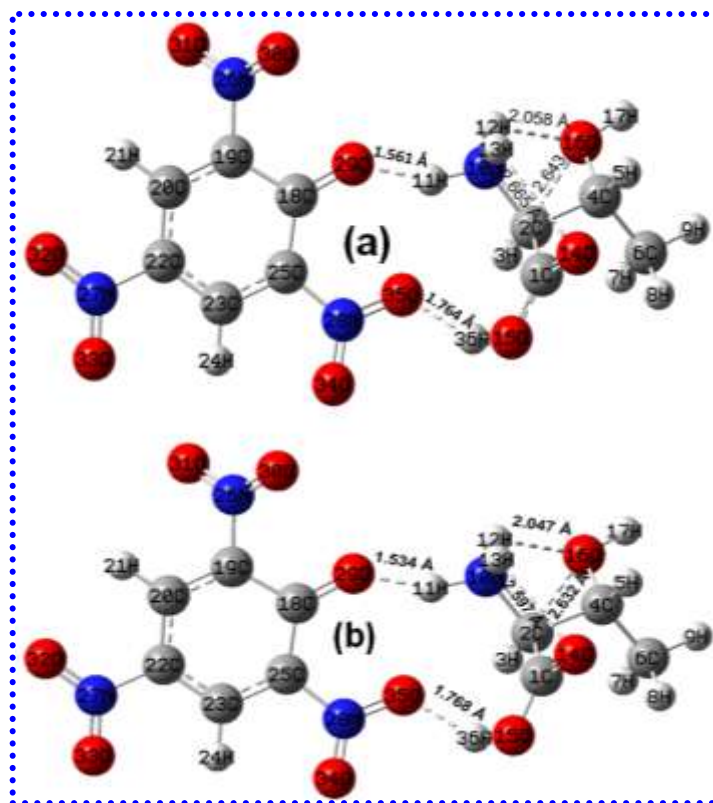


Fig. 1. Optimized ground state geometry of L-threonine picrate (LTHP) obtained with (a) B3LYP and (b) CAM-B3LYP using 6-31G* basis set.

Table 1 The calculated bond lengths and bond angles of LTHP optimized molecule by DFT/B3LYP using 6-31G* level of theory

Bond lengths	Cal. (Å)	Bond Angles	Cal. (°)	Bond lengths	Cal. (Å)	Bond Angles	Cal. (°)
L-threonine cation				Picrate anion			
C1-O14	1.0196	O14-C1-O15	123.322	C18-O29	1.2525	C19-C18-O29	121.093
C1-O15	1.3126	O14-C1-C2	119.037	C18-C19	1.4598	C25-C18-O29	126.404
C1-C2	1.2140	C1-C2-H3	112.946	C19-N26	1.4680	C19-N26-O30	118.164
C2-H3	1.5420	H3-C2-N10	106.083	N26-O30	1.2277	C19-N26-O31	117.005
C2-C4	1.0888	C2-N10-H11	114.615	N26-O31	1.2336	C19-C20-H21	120.367
C4-H5	1.0917	C2-N10-H12	107.237	C19-C20	1.3715	H21-C20-C22	120.203
C4-C6	1.5076	C2-N10-H13	110.411	C20-H21	1.0827	C22-N27-O32	117.456
C6-H7	1.0313	C2-C4-H5	107.937	C20-C22	1.4047	C22-N27-O33	117.786
C6-H8	1.0229	C2-C4-C6	111.943	C22-N27	1.4573	C22-C23-H24	120.172
C6-H9	1.0625	H5-C4-O16	110.410	N27-O32	1.2326	C22-C23-C25	119.889
C4-O16	1.0955	C4-C6-H7	110.727	N27-O33	1.2325	C24-C23-C25	119.980
O16-H17	0.9694	C4-C6-H8	111.036	C22-C23	1.3803	C23-C25-N28	115.720
C2-N10	1.5004	C5-C6-H9	110.124	C23-H24	1.0820	O25-N28-O34	120.246
N10-H11	1.0822	C2-C4-O16	104.129	C23-C25	1.3972	O25-N28-O35	118.405
N10-H12	1.0295	C4-O16-H17	108.870	C25-N28	1.4305	C18-C25-N28	121.240
N10-H13	1.0258	C4-C2-N10	108.630	N28-O34	1.2290		
				N28-O35	1.2600		

The Mulliken charge in any molecule is directly related to their vibrational properties and quantifies how the electronic structure charges under atomic displacement. Therefore it is directly related to the chemical bonds present in the titled molecule. It affects many parameters of the molecule such as its dipole moment, polarizability, electronic structure and other properties of molecular system [31, 32]. The net atomic charges of LTHP molecule in ground state are tabulated in Table S1 and also shown in Fig. S1 (see supplementary data). While all the hydrogen atoms in the molecule have positive charges and very similar negative charges are noticed for the oxygen atoms. The carbon atom C(1) acquire maximum positive charge due to its bonding with two electronegative oxygen atoms O(14) and O(15) [33, 34]. It is important to mention here that N(10) atom has the maximum negative charge because may be it draws charge from its adjacent hydrogen atoms.

3.2. Vibrational analysis

L-Threoninium picrate ($C_{10}H_{12}N_4O_{10}$) crystallize in the monoclinic non-centrosymmetric space group *P*21 (*Z*=2) with unit cell dimensions $a = 9.235(5) \text{ \AA}$, $b = 6.265(5) \text{ \AA}$, $c = 12.727(5) \text{ \AA}$, $\beta = 108.42(5)^\circ$ and cell volume $698.6(7) \text{ \AA}^3$ [16]. The unit cell comprises *L*-threoninium cations and picrate anions (Fig. 1). *L*-threoninium cation has carboxyl (-COOH), a protonated NH_3^+ , methyl and alcoholic -OH groups while picrate anion has o- and p- substituted nitro (-NO₂), alcohol (-OH) groups and phenyl ring. The loss of H in the picrate anion is confirmed by the C-C distances near the phenolic group (C5-C6 and C5-C10). The picrate anion forms a strong asymmetric intermolecular; O-H...O and N-H...O hydrogen bonds with the threonine cation. Out of the three nitro groups, two (N2/O5/O6 and N4/O9/O10) present at ortho-positions w.r.t. C-OH group which are twisted from the plane of ring. While, C-N twisting vibration is not C-N bond length dependent [35]. The molecular structure proposed by Natarajan et al. of LTHP is presented in Fig. 1. Intermolecular N1-H1C...O1 hydrogen bonding interaction form a linear zigzag head-to-tail chain of amino acid. These linear chains propagates along the b-axis which are separated by picrate anions on either side through O2-H2...O4 inter-molecular hydrogen bonding interaction. An intra-molecular hydrogen bonds are formed between the amine N atom and the nearby oxygen atom, e.g. N1-H1B...O3 and within different zigzag structures of chain. The vibrational (IR and Raman) spectroscopy play a vital role in revealing the structural details of organic, inorganic and hybrid compounds from the appearance of different fundamental vibrational modes of basic skeletal and functional groups present in a material. In organic compounds, the conformational arrangement of molecular groups sometimes may lead to shifting of some peak positions to higher or lower frequencies with gain or loss in intensity. Theoretically, IR and Raman spectra of LTHP molecule are derived by B3LYP and HF

approaches using 6-31G* basis set are presented Figs. 2 (a-c) and 3 (a-c), respectively. The observed IR and Raman peaks of LTHP functional groups and skeletal molecule are tentatively assigned on the basis of earlier reported available data on amino acids and picrate compounds [36, 37]. Due to the combination of electron correlation effects and basis set deficiencies, the calculated harmonic frequencies are found to be higher than the experimentally observed frequencies. So, for 6-31G* basis set of B3LYP and HF the scaling factor 0.9613 and 0.8929 were used, respectively. Table S2 (see supplementary data) shows all the calculated frequencies and their tentative assignments which are in well correlation with the reported values on such type of picrate compounds [16, 37, 38]. The O-H bond in phenol of picrate is broken down and the hydrogen is attracted by the N of the amino group to form NH_3^+ in L-Threonine. The removal hydrogen from O-H group, the double bond is created between C and O forms C=O.

In 3400 – 3000 cm^{-1} Region

In amino acid, -OH group stretching vibrations are generally observed around 3500 cm^{-1} . Their peak positions are very sensitive to the environment and exhibit pronounced shift due to hydrogen bonded species. The asymmetric stretching vibrational mode of O-H group appear as medium to strong intensity broad band in IR spectrum. In these spectra, a strong O-H stretching mode band appeared at 3340 cm^{-1} (B3LYP), 3348 cm^{-1} (HF) in the IR spectra and at 3334 cm^{-1} (B3LYP), 3348 cm^{-1} (HF) in Raman spectra. This mode is merged with the $-\text{NH}_2$ asymmetric stretching mode and both appeared at the same position. In IR transmission spectra, N-H asymmetric and symmetric stretching modes of amine ($-\text{NH}_2$) group appear as strong and medium intensity peaks at 3340 cm^{-1} and 3271 cm^{-1} (B3LYP) and at 3348 cm^{-1} and 3276 cm^{-1} (HF), respectively. While in Raman spectra these modes are obtained as weak intensity peaks at 3334 cm^{-1} and 3265 cm^{-1} (B3LYP) and at 3348 cm^{-1} and 3277 cm^{-1} (HF). The asymmetric stretching vibration $-\text{NH}_3^+$

cation is expected in 3200-3100 cm^{-1} region; in *LTHP* crystal IR and Raman spectra at B3LYP is obtained as weak intensity peak at 3150 cm^{-1} and 3135 cm^{-1} , respectively. C-H asymmetric and symmetric stretching vibration modes of aromatic benzene ring are observed for e_{2u} symmetry vibrations at 3037 cm^{-1} , 3011 cm^{-1} (B3LYP) and a_{1g} non-degenerate symmetry vibration at 3089 cm^{-1} (HF) in theoretical IR transmission spectra and for e_{2g} symmetry vibration at 3031 cm^{-1} (B3LYP), 3090 cm^{-1} (HF) of a_{1g} symmetry vibration in Raman spectra of this crystal [39, 40]. The methyl (-CH₃) group asymmetric stretching mode is observed at 2920 cm^{-1} (B3LYP) and only symmetric stretching mode at 2837 cm^{-1} (HF) in IR transmission spectra while in Raman spectra, asymmetric and symmetric stretching modes are obtained at 2945 cm^{-1} and 2884 cm^{-1} (B3LYP) and only asymmetric stretching mode at 2980 cm^{-1} .

In 2000 - 1300 cm^{-1} region

In this region, the tentative vibrations of carbonyl (-COOH) group stretching modes, protonated amino (NH₃), amino (-NH₃⁺) cation and methyl deformation modes, nitro (-NO₂) group stretching modes are observed. The carbonyl -C=O stretching mode is observed as strong peak at 1780 cm^{-1} (B3LYP), 1810 cm^{-1} (HF) infrared transmission spectrum and at 1777 cm^{-1} (B3LYP), 1812 cm^{-1} (HF) as weak band in Raman spectra of this sample. The large shift in the peak position as compared to amino acid carbonyl -C=O mode which is expected to occur at ~ 1740 cm^{-1} to higher wavenumbers reflects the existence of strong hydrogen bonding among different available functional groups in crystal lattice. The strong medium intensity -NH₃⁺ deformation band and -C=C- ring vibration is observed in IR transmission spectra at 1633 cm^{-1} (B3LYP), 1678, 1642 (HF) cm^{-1} and in Raman spectra at 1630 cm^{-1} (B3LYP), 1770 (HF) cm^{-1} . As we know that aromatic nitro compounds have strong absorption due to asymmetric stretching vibration of the NO₂ group at 1570-1485 cm^{-1} . Hydrogen bonding has a minor effect on the -NO₂

asymmetric stretching vibrations [41, 42]. In the present case, very strong bands of $-\text{NO}_2$ asymmetric stretching mode is observed at 1607 cm^{-1} (B3LYP), 1578 cm^{-1} (HF) in IR transmission spectra and at 1605 cm^{-1} (B3LYP), 1580 cm^{-1} (HF) in Raman spectra as weak peak components. The shifting of this mode to higher frequency confirms the realignment of the vibrations due to the inductive effect of H of Phenol. The NH_3 symmetric deformation mode is observed in IR transmission spectrum at 1546 cm^{-1} (B3LYP) and 1535 cm^{-1} (HF) as a very strong peak while in Raman spectra this medium intensity peak has two components at 1561 , 1543 cm^{-1} (B3LYP) and 1540 , 1535 cm^{-1} (HF). The N-H deformation vibrations are moved down to low wavenumber as these modes are affected by other nearby vibrations. DFT theoretical calculations showed that in aliphatic compounds with $-\text{CH}_3$ group, the series of bands are obtained pertaining to asymmetric and symmetric deformation modes in the region 1500 - 1400 cm^{-1} [43-45]. These modes mainly from coupling of C-H and C-C stretching vibrations of deformed $-\text{CH}_3$ group. In the present investigation, $-\text{CH}_3$ asymmetric deformation mode is observed as medium intensity band at 1492 cm^{-1} (B3LYP), 1465 (HF) in IR transmission spectra while at 1509 , 1465 cm^{-1} (B3LYP) and 1509 , 1465 cm^{-1} as weak bands in Raman bands are assigned as the asymmetric and symmetric deformation modes of methyl group. The presence of these bands exhibits the existence $-\text{CH}_3$ groups at different environment in crystal lattice. As it is well-known that aromatic nitro compounds have strong absorptions to asymmetric and symmetric stretching vibrations of the $-\text{NO}_2$ group at ~ 1450 and 1325 cm^{-1} , respectively. Hydrogen bonding has a minor effect on the $-\text{NO}_2$ asymmetric stretching vibrations. In the present case, $-\text{NO}_2$ asymmetric stretching weak bands have been observed at 1416 , 1398 cm^{-1} (B3LYP), 1437 , 1400 cm^{-1} (HF) in IR transmission spectra and at 1414 cm^{-1} (B3LYP) and 1437

cm^{-1} (HF) Raman spectra. The symmetric stretching modes of $-\text{NO}_2$ are obtained as very strong peaks at 1347, 1330, 1312 cm^{-1} (B3LYP), 1338 (HF) in IR transmission spectra and at 1344, 1327 (B3LYP), 1339 (HF) Raman spectra. The presence of three peaks in B3LYP IR spectrum shows that nitro group acquire different environment or site symmetry in lattice. Their peak positions are sensitive to hydrogen bonding which may cause rearrangement through the inductive effect of H of phenol [46-48].

In 1300 – 1000 cm^{-1} region

In this region, $-\text{CH}_3$ group deformation mode, C-O of phenolic group and C-OH, C=O, C=C groups symmetric stretching modes are observed as strong and medium intensity bands. A medium intensity peak at 1278 cm^{-1} (B3LYP), 1223 cm^{-1} (HF) in IR transmission spectra and in Raman spectra as weak peaks at 1310, 1275 cm^{-1} (B3LYP), 1225 cm^{-1} (HF), respectively are observed in these spectra. These peaks are emerged from the $-\text{CH}_3$ group deformation and -C-O phenol and -C-OH amino acid alcohol group symmetric stretching vibrations in the crystal. The medium intensity -C=O and -C=C- symmetric stretching vibrational peaks are obtained at 1165, 1140 cm^{-1} (B3LYP), 1190, 1151 cm^{-1} (HF) and 1096, 1061 cm^{-1} (B3LYP), 1080 cm^{-1} in IR transmission spectra respectively while these modes appear at 1170, 1137 cm^{-1} (B3LYP), 1160 cm^{-1} (HF). In Raman spectra, these -C=O and -C=C- symmetric stretching mode peaks are obtained as very weak and weak intensity peaks at 1170, 1137 cm^{-1} (B3LYP), 1160 cm^{-1} (HF) and 1093 cm^{-1} (B3LYP), 1080 cm^{-1} (HF) respectively. The two components in these stretching modes suggest that these two groups are present in different sites of crystal lattice.

In 1000 – 400 cm^{-1} region

This region is comprised of the stretching vibrations of C-C ring, C-C skeletal, $-\text{NO}_2$ scissoring, bending, C-H bending, COO-, C-C-N deformation and $-\text{NO}_2$ bending modes. The C-C ring and

skeletal stretching modes has been noticed as weak and very weak peaks at 905 cm^{-1} (B3LYP), 930 cm^{-1} (HF) and 818 cm^{-1} (B3LYP), 792 cm^{-1} (HF), respectively in IR transmission spectra. In Raman spectra these C-C ring and skeletal stretching modes are obtained as medium intensity peaks at 929, 903, 860 cm^{-1} (B3LYP), 946 cm^{-1} (HF) and 834, 799, 707 cm^{-1} (B3LYP), 723 cm^{-1} (HF) respectively. The $-\text{NO}_2$ scissoring mode appears as weak and very weak components at 766 cm^{-1} (B3LYP), 741, 714 cm^{-1} (HF) IR spectra and at 747, 721, 707 cm^{-1} (B3LYP), 723 cm^{-1} (HF) in Raman spectra. The $-\text{NO}_2$ bending, $-\text{C}-\text{H}$ bending, $-\text{COO}-$ deformation modes appear at 705, 698 cm^{-1} (B3LYP), 696 cm^{-1} (HF) in IR spectra and as very weak components at 678, 661, 644 cm^{-1} (B3LYP), 698 cm^{-1} (HF) in Raman spectra. Aromatic nitro compounds have a band of weak to medium intensity in the region 590–500 cm^{-1} [45] due to the out-of-plane bending deformations mode of NO_2 group. In IR transmission spectrum, the rocking (out-of-plane bending deformation) vibration of $-\text{NO}_2$ has been observed at 575 cm^{-1} (B3LYP) as medium intensity peak and in Raman spectrum this peak appears as weak intensity peak at 574 cm^{-1} (B3LYP). The C-C-N in-phase deformation mode is observed as weak intensity peak at 532 cm^{-1} (B3LYP), 553 cm^{-1} (HF) in IR transmission spectrum and at 532 cm^{-1} (B3LYP), 533 cm^{-1} (HF) in Raman spectra. Carboxylate (COO^-) anion rocking vibration is obtained at 427 cm^{-1} (B3LYP) IR transmission and Raman Spectra as a weak intensity feature.

In 400 -10 cm^{-1} region

This is far infrared (FIR) region in which the lattice vibrations are obtained. In these, (B3LYP and HF) IR transmission and Raman spectra, the medium and weak intensity vibrational peaks are obtained. The C-C-N out-of-plane bending and skeletal vibrations are found at 385, 360 and 340 cm^{-1} as medium and weak intensity components in (B3LYP), 366, 321 cm^{-1} (HF) in IR transmission spectra. While in Raman spectra, these modes appear as weak and medium intensity

peak components at 384, 367, 323 cm^{-1} (B3LYP), 366, 321 cm^{-1} (HF). The shift in out-of-phase vibrations of skeletal carbon to low wavenumber i.e. $\sim 320 \text{ cm}^{-1}$ is attributed to the repulsion between the $-\text{NO}_2$ groups. The C-CH_3 in-plane bending vibration is obtained at 280 (weak), 263 (medium) cm^{-1} (B3LYP), 267 cm^{-1} (HF) in IR transmission spectra. In Raman spectra, this weak peak is observed at 263 cm^{-1} (B3LYP). While C-CH_3 out-of-plane bending vibration is obtained as weak intensity band in IR transmission spectra at 203 cm^{-1} (B3LYP), 196 cm^{-1} (HF) and as weak intensity components in Raman spectra at 194, 150 cm^{-1} (B3LYP) and 196 cm^{-1} (HF). The deviation in peak position of these vibrations indicates the repulsion between methyl groups. $-\text{NO}_2$ twisting vibrations are observed at 60, 50 and 40 cm^{-1} . In these IR transmission spectra, these modes appear as very, very weak (vww) components while in Raman B3LYP spectrum, 60 (vww) and 50 (w) cm^{-1} components are observed. It means one band of in-plane bending pushed up and entire bands of out of plane bending are within the region mainly due to OH group. This in-depth IR transmission and Raman theoretical spectra from 4000-10 cm^{-1} region analysis revealed the existence of *L*-threoninium and picric acid salt in ionic as well as in covalent state. These spectra showed all the peaks of functional and skeletal groups present in the crystal lattice. All the observed modes are tentatively assigned on the basis earlier reported results and available literature. The presence of hydrogen bonding cause shifting of peaks to higher or lower wavenumbers depending upon the electron inductive or withdrawing nature of the bonded functional groups present in the crystal.

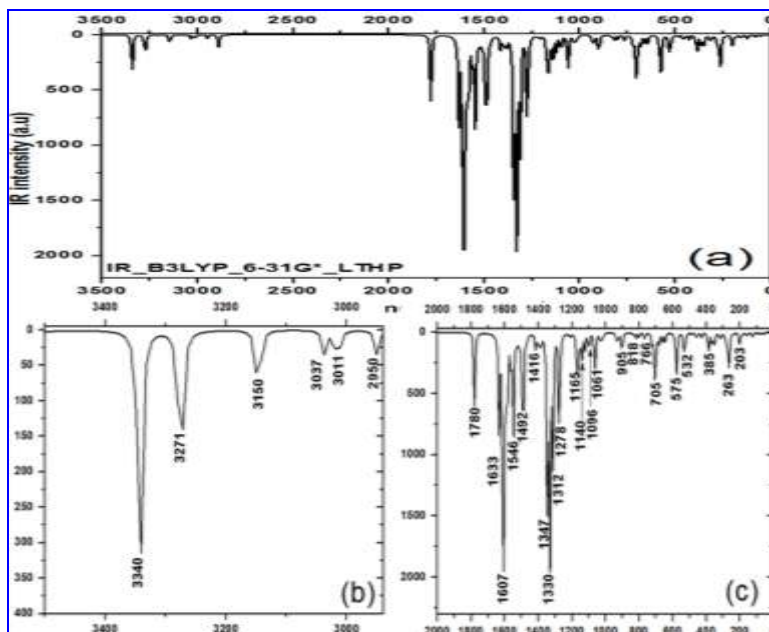


Fig. 2. Calculated IR spectra of L-threonine picrate (LTHP) molecule at B3LYP/6-31G* level of theory.

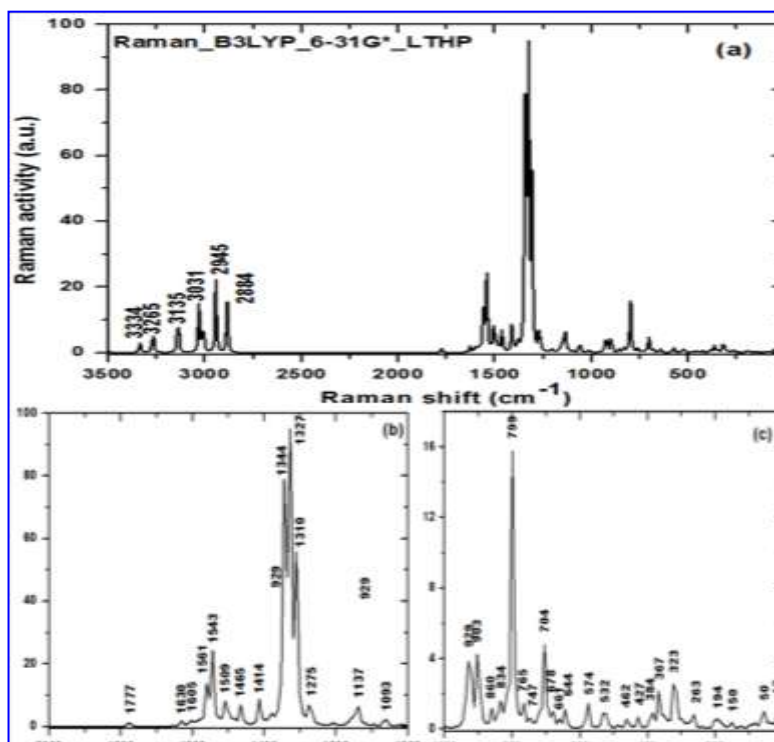


Fig. 3. Calculated Raman spectra of L-threonine picrate (LTHP) molecule at B3LYP/6-31G* level of theory.

3.3. Electro-optical properties

3.3.1. UV-Vis spectral analysis (TD-DFT Study)

Nowadays the time dependent range separated density functional theory is the most popular method for ground state electronic structure calculations in quantum chemistry and solid state physics [20, 21]. When compared to traditional ab initio and semi-empirical approaches the contemporary density functional methods show a favorable balance between accuracy and computational efficiency.

To analyze the nature of electronic transition in LTHP molecule the TD-DFT TD-B3LYP/6-31G* and range separated functionals CAM/B3LYP/6-31G* and LC-BLYP/6-31G* levels of theory. Fig. 4 shows the calculated UV-Vis spectra of LTHP molecule using different functionals such as B3LYP, LC-BLYP and CAM-B3LYP using 6-31G* basis set. Fig. 4 shows two absorption maxima at 210 and 281 nm calculated at TD-B3LYP/6-31G* level of theory. However, these values dramatically changed when we used range separated functionals such as LC-BLYP and CAM-B3LYP which are found to be 237, 323 nm and 262, 351 nm, respectively. The calculated values from CAM-B3LYP are found to be very close to the experimental results [16]. Optimized geometry of LTHP molecule represents that the maximum absorption wavelength is due to the electronic transition from HOMO to LUMO which will be explained in the next section. The observed bands are due to $\pi - \pi^*$ and $n - \pi^*$ transitions and in the chemical stability of LTHP molecule both HOMO and LUMO are taking participation.

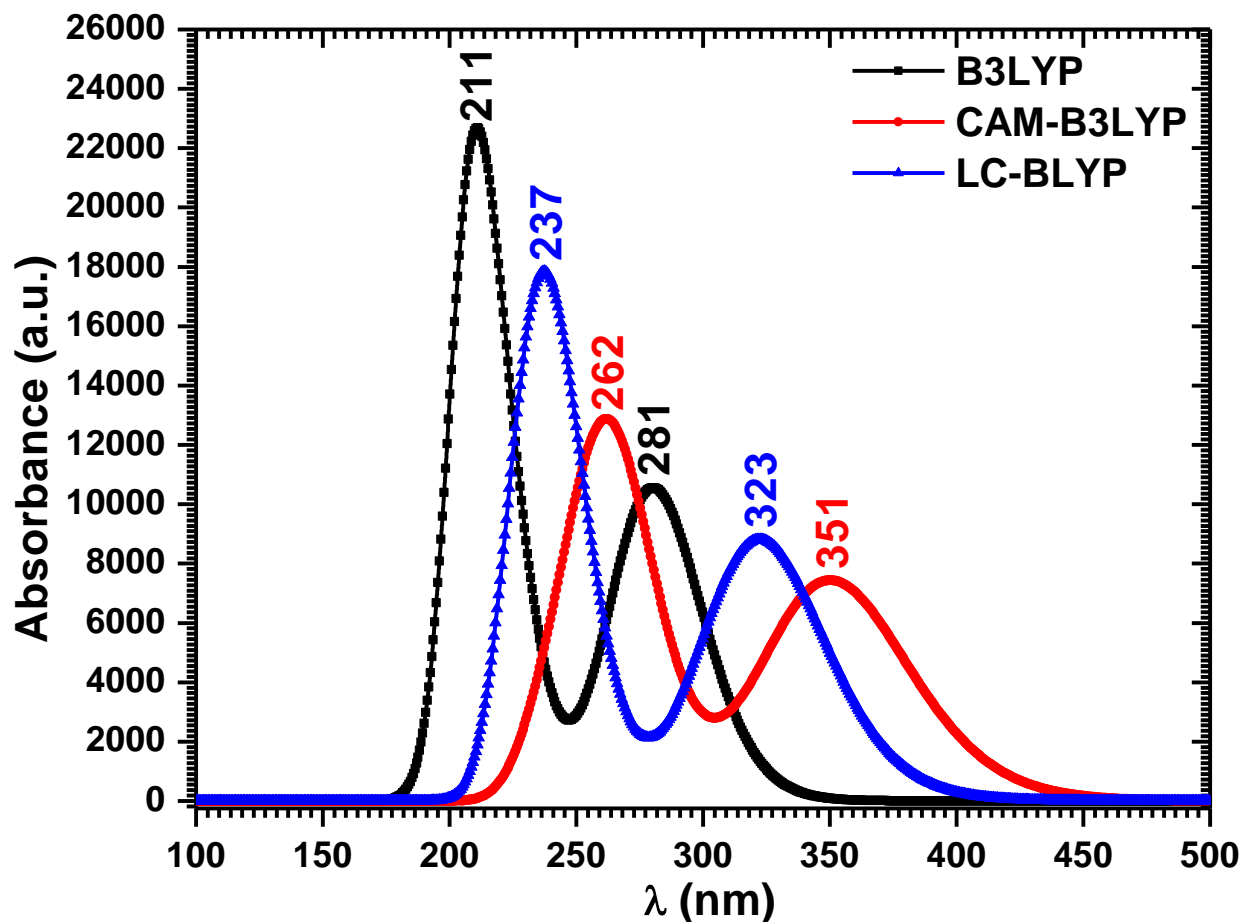


Fig 4. Calculated UV-Visible spectra of LTHP molecule at different levels of theory.

3.3.2. *Electronic properties*

The frontier molecular orbitals (FMOs) such as HOMO and LUMO, represents the ability to donate or accept the electrons, respectively in any compound which plays important role in its electrical and optical properties as well as chemical reactions. The chemical hardness, potential, reactivity, softness, electronegativity, electrophilicity, kinetic stability and optical Polarizability, etc. of any molecule can be explained with the help of HOMO and LUMO energies. The energy values of HOMO and LUMO orbitals calculated by B3LYP using 6-31G* basis set are presented in Table S3 (see supplementary data).

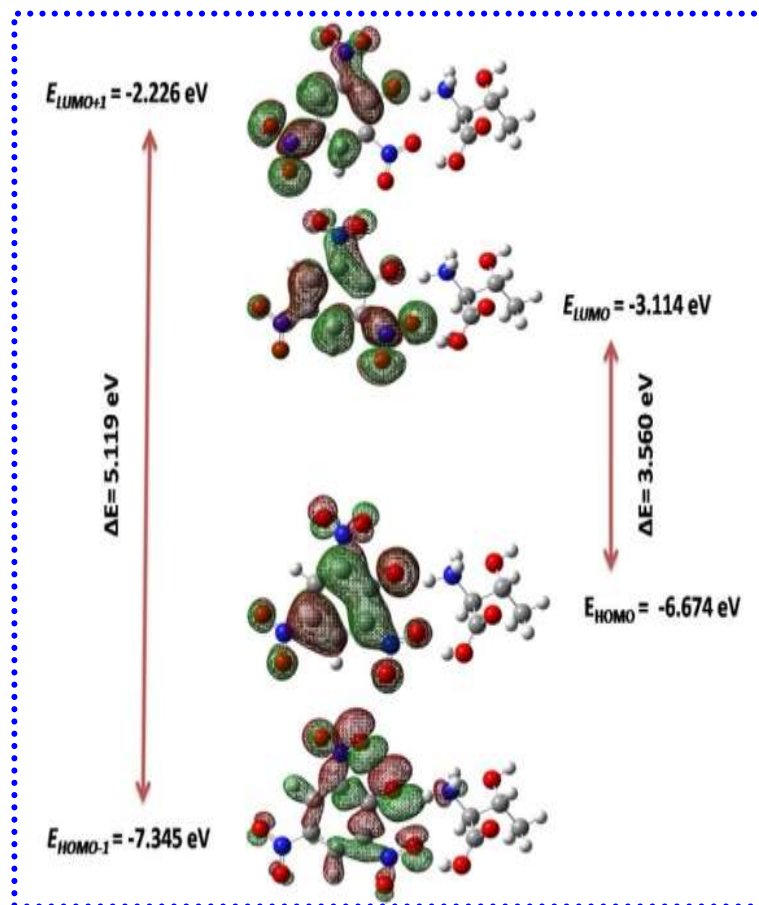


Fig 5. The HOMO, HOMO-1, LUMO and LUMO+1 representation and charge density distribution of LTHP molecule calculated at B3LYP/6-31G* level of theory.

The atomic orbital composition of the FMOs are sketched and shown in Fig. 5. From the Fig. 5, it is clear that the HOMO and LUMO both are distributed on picrate anion. From the Mulliken charge analysis it is also clear that the charge transfer take place mainly within the picrate anion upon excitation. The density of states (DOS) play vital role to understand the energy spectrum especially the electron distribution. To shed light on the electronic band structure of LTHP, we also studied the total/partial DOS (T/PDOS) using GGA/BLYP and presented in Fig. 6. In LTHP, the energy band in the bottom of valence band (VB) at ~ -18.5 to -19.0 , -14.0 Hartree, the middle of VB at ~ -9.5 to -10.0 Hartree is defined by the *s*-orbitals. Moreover, the *s*-orbitals

further appear in the upper VB and conduction band (CB) in the energy range of 0 to -1.0 and 0 to 0.4 Hartree, respectively, which reveals the negligible contribution of *s*-orbitals into the electronic properties of DPNDF. The upper VB and CB in the energy range ~ 0 to -1.0 and 0 to 0.4 are only contributions from the *p*-orbitals. The DOS profiles of the LTHP shows the upper VB and CB are primarily of *s* and *p*-character.

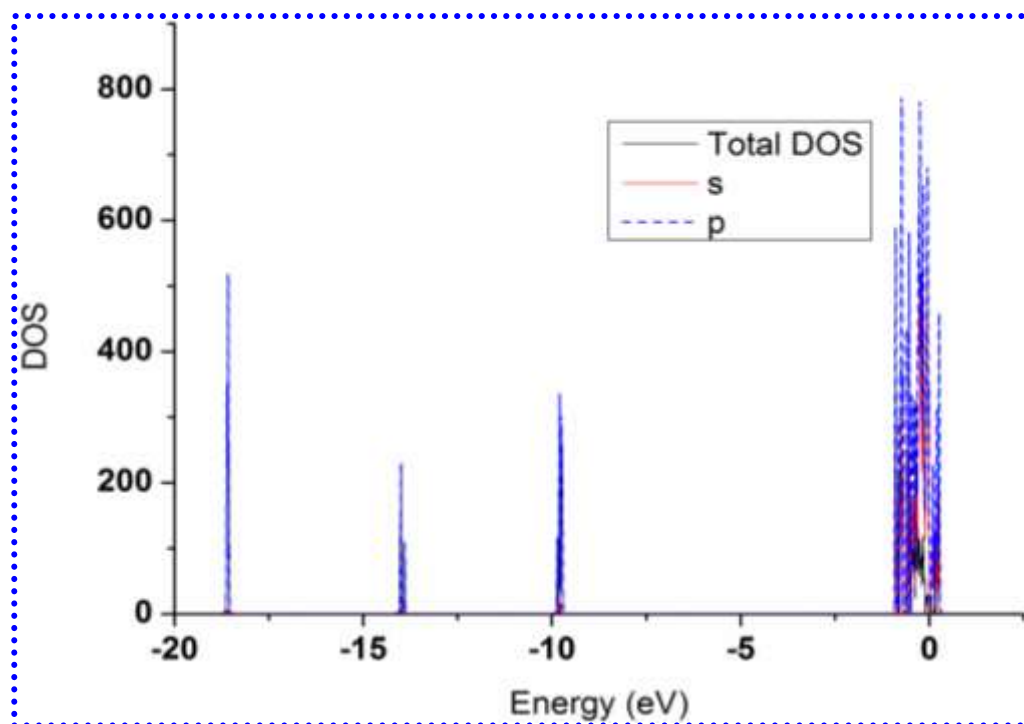


Fig. 6. Density of states of LTHP molecule.

The molecular electrostatic potential (MEP) mapping of LTHP has been illustrated in Fig. 7. The MEP is helpful property to investigate the reactivity of molecular species by predicting the possible site for nucleophile and electrophilic attack. In MEP plot, while maximum positive region that is preferred site for nucleophilic attack indicated as blue color. Similarly, a maximum negative region is preferred site for electrophilic attack that is indicated as red surface. The TED plots of the titled molecule show a uniform distribution.

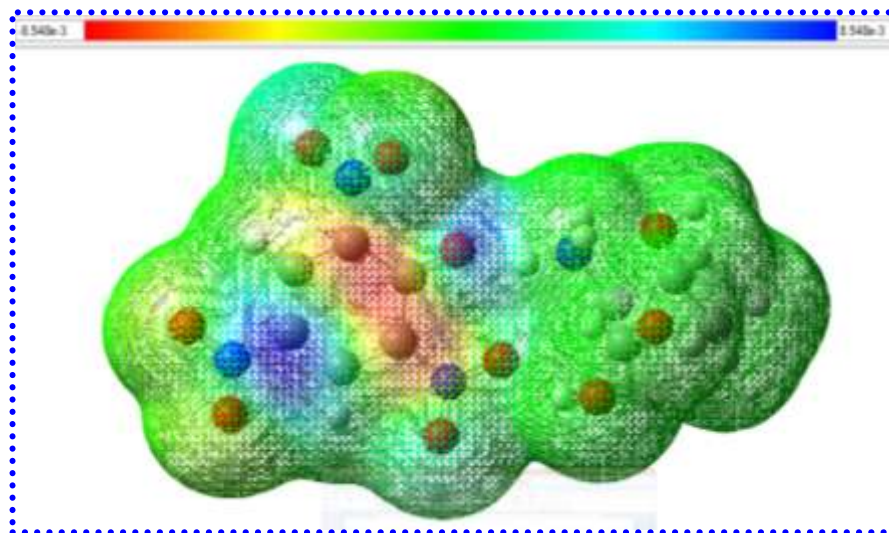


Fig. 7. Molecular electrostatic potential (MEP) map of LTHP molecule at ISO value 0.02.

Global chemical reactivity descriptors (*GCRD*) are based on the conceptual DFT and are used to understand the relationship between global chemical reactivity, structure, stability etc. parameters of any molecule. Additionally, these descriptors are also employed in the progress of quantitative structure-activity (QSAR), quantitative structure-property (QSPR), and quantitative structure-toxicity (QSTR) relationships. The hardness of any molecule is related to aromaticity [49]. The DFT provides the definitions of important universal concepts of molecular structure stability and reactivity [50]. Here our focus is to find the values of various GCRD parameters such as chemical hardness (η), chemical potential (μ), softness (S), electronegativity (χ) and electrophilicity index (ω) of LTHP molecule using HOMO and LUMO energies values using different functionals which are given in Table S3 (see supplementary data). The calculated HOMO-LUMO energy gap and chemical hardness values show that the titled molecule possesses good chemical stability. The larger energy gap suggests that the LTHP has significant kinetic stability as according to softness-hardness rule when the molecule possesses wide energy gap then said to be hard and also show higher thermal and kinetic stability.

3.4. Polarizability and first hyperpolarizability studies

Nonlinear activity of any materials provides the key functions from applications point of views for frequency shifting, optical modulation, optical switching etc. for developing technologies in the area of communication, optical processing and interconnection [51, 52]. It is well known that the importance of polarizability and hyperpolarizability of a molecular system is dependent on the electronic communication of two different parts of a molecule. There are many reports available on the choice of suitability of functional for nonlinear optical parameter calculations [20, 21, 53, 54]. We have chosen the various functionals like: B3LYP and range separated CAM-B3LYP, LC-BLYP using 6-31G* basis set and various parameters such as electronic dipole moment (μ), total average polarizability (α_0), anisotropy of polarizability ($\Delta\alpha$) and static first hyperpolarizability (β_{tot} ; β_0) have been calculated and presented in Table 2 (computational details can be found in supporting information) and also the variation of μ_{tot} and β_{tot} calculated by above mentioned methods with respect to urea is shown in Figure 2S(a) and (b) [see supporting information].

The value of total dipole moment (μ_{tot}) and first hyperpolarizability is found to be 3 and 51 times higher than urea ($\mu_{Urea} = 4.24$ Debye, $\beta_{tot} = 0.22 \times 10^{-30}$ esu.) molecule calculated at B3LYP/6-31G* level of theory [55] as well as many other compounds [56-63], while experimentally the second harmonic generation of the titled compound in solid form was measured by S. Natarajan et al., and found to be 43 times higher than KDP molecule [16]. Such high nonlinearity recommended the titled compound for optoelectronic and electro-optic device applications.

Table 2 Calculated values of polarizabilities, dipole moments and hyperpolarizability along with their individual tensor components by DFT/B3LYP, CAM-B3LYP and LC-BLYP using /6-31G* basis set of LTHP molecule.

<i>Polarizabilities and dipole moments</i>							<i>Hyperpolarizabilities</i>						
	<i>B3LYP</i>		<i>CAM-B3LYP</i>		<i>LC-BLYP</i>			<i>B3LYP</i>		<i>CAM-B3LYP</i>		<i>LC-BLYP</i>	
	<i>a.u.</i>	<i>esu</i> ($\times 10^{-24}$)	<i>a.u.</i>	<i>esu.</i> ($\times 10^{-24}$)	<i>a.u.</i>	<i>esu.</i> ($\times 10^{-24}$)		<i>a.u.</i>	<i>esu</i> ($\times 10^{-30}$)	<i>a.u.</i>	<i>esu.</i> ($\times 10^{-30}$)	<i>a.u.</i>	<i>esu.</i> ($\times 10^{-30}$)
α_{xx}	264.989	39.271	249.916	37.038	239.668	35.519	β_{xxx}	-616.094	-5.316	-469.490	-4.051	-395.264	-3.411
α_{xy}	2.697	0.399	2.837	0.421	3.2705	0.485	β_{xxy}	-789.778	-6.815	-729.921	-6.298	-707.328	-6.104
α_{yy}	200.641	29.735	192.177	28.481	186.106	27.581	β_{xyy}	131.381	1.134	167.528	1.446	213.629	1.844
α_{xz}	9.811	1.454	9.397	1.393	9.522	1.411	β_{yyy}	345.620	2.982	271.682	2.344	206.938	1.786
α_{yz}	5.648	0.837	5.343	0.792	5.072	0.752	β_{xzz}	-111.222	-0.960	-91.173	-0.787	-81.141	-0.7
α_{zz}	97.191	14.404	95.708	14.184	94.532	14.01	β_{yyz}	-68.439	-0.591	-57.278	-0.495	-51.170	-0.442
α_{tot}	187.607	27.803	179.267	26.567	173.435	25.703	β_{yzz}	48.124	0.415	38.025	0.328	35.725	0.308
$\Delta\alpha$	147.608	21.876	135.922	20.144	128.186	18.997	β_{zzz}	-5.413	-0.047	-5.871	-0.051	-5.149	-0.045
μ_x	4.605	11.697D	4.530	11.514D	4.535	11.528D	β_{zzz}	7.095	0.061	1.713	0.015	0.660	0.006
μ_y	0.781	1.980D	0.692	1.758D	0.651	1.656D	β_{zzz}	-22.020	-0.190	-16.955	-0.146	-14.665	-0.127
μ_z	-1.116	-2.835D	-1.142	-2.903D	-1.175	-2.988D	β_0	783.353	6.760	632.898	5.642	542.233	4.679
μ_{tot}	4.80	12.20D	4.723	12.003D	4.729	12.023D	β_{tot}	1305.588	11.266	1054.981	9.103	903.721	7.798

For α , 1 a.u. = 0.1482×10^{-24} esu, for β , 1 a.u. = 0.008629×10^{-30} esu, $\mu_{Urea} = 4.24D$ and $\beta_{Urea} = 0.22 \times 10^{-30}$ esu [55]

4. Conclusions

The strong hydrogen bonding was observed between picric acid and L-threonine. The proton transfer from picric acid to L-threonine is confirming the formation of L-threoninium picrate compound. The HF and B3LYP calculated infrared and Raman frequencies were assigned and compared with the experimental values and found to be in close approximation. The dipole moment (μ_{tot}), polarizability (α_0) and first hyperpolarizability (β_{tot}) values were calculated at different levels of theory. The β_{tot} value was found to be 51 times higher than urea computed at same level of theory. Two absorption bands were observed in UV-Vis spectra at all the applied

methods. The absorption bands calculated using range separated functional CAM-B3LYP were found at 262 and 351 nm. The total/partial DOS (T/PDOS) was determined using GGA/BLYP. The chemical reactivity descriptors show that LTHP has significant chemical stability. The molecular electrostatic potential map gives the information about nucleophilic attack electrophilic attack in the molecule. Such high nonlinear property of LTHP molecule suggest that it is a good candidate for higher order nonlinear applications and also may help to the scientists and researchers in design and synthesis of new materials with unique optical properties as well.

Acknowledgment

The authors are thankful to King Khalid University, Abha, Saudi Arabia for providing research infrastructure. The authors are also thankful to Dr. I.S. Yahia, Nano-Science & Semiconductor Labs., Faculty of Education, Ain Shams University, Roxy, Cairo, Egypt, for supporting the calculations with Gaussian software.

References

- [1] B. Saleh, MC Teich Fundamentals of photonics, in, New York: John Wiley & Sons, 1991.
- [2] B.G. Penn, B.H. Cardelino, C.E. Moore, A.W. Shields, D. Frazier, Growth of bulk single crystals of organic materials for nonlinear optical devices: An overview, Progress in Crystal Growth and Characterization of Materials, 22 (1991) 19-51.
- [3] M. Shakir, B. Singh, B. Kumar, G. Bhagavannarayana, Ferroelectricity in glycine picrate: An astonishing observation in a centrosymmetric crystal, Applied Physics Letters, 95 (2009) 252902-252902-252903.
- [4] Mohd. Shakir, G. Bhagavannarayana, B. K. Singh, Binay Kumar, Organic ferroelectrics: A big surprise, NPG Asia Materials, (2010).
- [5] M. Ravi, P. Gangopadhyay, D.N. Rao, S. Cohen, I. Agranat, T.P. Radhakrishnan, Dual Influence of H-Bonding on the Solid-State Second- Harmonic Generation of a Chiral Quinonoid Compound, Chemistry of Materials, 10 (1998) 2371-2377.
- [6] P. Franken, J. Ward, Optical harmonics and nonlinear phenomena, Reviews of Modern Physics, 35 (1963) 23.
- [7] J.M. Cole, C.C. Wilson, J.A. Howard, F.R. Cruickshank, Quantitative analysis of hydrogen bonding and atomic thermal motion in the organic non-linear optical material DCNP using X-ray and neutron diffraction, Acta Crystallographica Section B: Structural Science, 56 (2000) 1085-1093.
- [8] J. Zyss, J. Nicoud, M. Coquillay, Chirality and hydrogen bonding in molecular crystals for phase-matched second-harmonic generation: N-(4-nitrophenyl)-(L)-prolinol (NPP), The Journal of chemical physics, 81 (1984) 4160-4167.

- [9] I. Ledoux, J. Badan, J. Zyss, A. Migus, D. Hulin, J. Etchepare, G. Grillon, A. Antonetti, Generation of high-peak-power tunable infrared femtosecond pulses in an organic crystal: application to time resolution of weak infrared signals, *JOSA B*, 4 (1987) 987-997.
- [10] A. Datta, S.K. Pati, Dipole orientation effects on nonlinear optical properties of organic molecular aggregates, *The Journal of chemical physics*, 118 (2003) 8420-8427.
- [11] M. Shakir, S. Kushwaha, K. Maurya, M. Arora, G. Bhagavannarayana, Growth and characterization of glycine picrate—Remarkable second-harmonic generation in centrosymmetric crystal, *Journal of crystal growth*, 311 (2009) 3871-3875.
- [12] T. KAI, M. GoTo, K. FURUHATA, H. TAKAYANAGI, Crystal structure of glycine picrate, *Analytical Sciences*, 10 (1994) 359-360.
- [13] P. Srinivasan, T. Kanagasekaran, R. Gopalakrishnan, G. Bhagavannarayana, P. Ramasamy, Studies on the Growth and Characterization of l-Asparaginium Picrate (LASP) A Novel Nonlinear Optical Crystal, *Crystal growth & design*, 6 (2006) 1663-1670.
- [14] M. Shkir, B. Riscob, G. Bhagavannarayana, Synthesis, growth, structural, spectroscopic, crystalline perfection, second harmonic generation (SHG) and thermal studies of 2-aminopyridinium picrate (2APP): A new nonlinear optical material, *Solid State Sciences*, 14 (2012) 773-776.
- [15] A. Aarthy, K. Anitha, S. Athimoolam, S.A. Bahadur, R. Rajaram, L-Asparaginium nitrate, *Acta Crystallographica Section E: Structure Reports Online*, 61 (2005) 2042-2044.
- [16] S. Natarajan, M. Umamaheswaran, J. Kalyana Sundar, J. Suresh, S.A. Martin Britto Dhas, Structural, spectroscopic and nonlinear optical studies on a new efficient organic donor–acceptor crystal for second harmonic generation: l-Threoninium picrate, *Spectrochimica Acta Part A: Molecular and Biomolecular Spectroscopy*, 77 (2010) 160-163.

- [17] A. Irfan, A.G. Al-Sehemi, A. Rasool Chaudhry, S. Muhammad, The structural, electro-optical, charge transport and nonlinear optical properties of oxazole (4Z)-4-Benzylidene-2-(4-methylphenyl)-1,3-oxazol-5(4H)-one derivative, *Journal of King Saud University - Science*, <http://dx.doi.org/10.1016/j.jksus.2016.10.004> (2016).
- [18] A. Irfan, A.G. Al-Sehemi, A.R. Chaudhry, S. Muhammad, A.M. Asiri, The structural, electro-optical, charge transport and nonlinear optical properties of 2-[(3,5-dimethyl-1-phenyl-1H-pyrazol-4-yl)methylidene]indan-1,3-dione, *Optik*, 127 (2016) 10148-10157.
- [19] M. Shkir, H. Abbas, Physico chemical properties of l-asparagine l-tartaric acid single crystals: A new nonlinear optical material, *Spectrochimica Acta Part A: Molecular and Biomolecular Spectroscopy*, 118 (2014) 172-176.
- [20] M.E. Foster, B.M. Wong, Nonempirically tuned range-separated DFT accurately predicts both fundamental and excitation gaps in DNA and RNA nucleobases, *Journal of chemical theory and computation*, 8 (2012) 2682-2687.
- [21] B.M. Wong, M. Piacenza, F. Della Sala, Absorption and fluorescence properties of oligothiophene biomarkers from long-range-corrected time-dependent density functional theory, *Physical Chemistry Chemical Physics*, 11 (2009) 4498-4508.
- [22] G.V. Gibbs, T.D. Crawford, A.F. Wallace, D.F. Cox, R.M. Parrish, E.G. Hohenstein, C.D. Sherrill, Role of Long-Range Intermolecular Forces in the Formation of Inorganic Nanoparticle Clusters, *The Journal of Physical Chemistry A*, 115 (2011) 12933-12940.
- [23] M. Shkir, S. AlFaify, H. Abbas, G. Bhagavannarayana, A physico-chemical approach to study the experimental and theoretical properties of l-ornithine monohydrochloride: An organic nonlinear optical material, *Materials Chemistry and Physics*, (2015).

- [24] M. Shkir, S. AlFaify, H. Abbas, S. Muhammad, First principal studies of spectroscopic (IR and Raman, UV-visible), molecular structure, linear and nonlinear optical properties of L-arginine p-nitrobenzoate monohydrate (LANB): a new non-centrosymmetric material, *Spectrochimica Acta Part A: Molecular and Biomolecular Spectroscopy*, (2015).
- [25] M. Shkir, S. Muhammad, S. AlFaify, Experimental and density functional theory (DFT): a dual approach to study the various important properties of monohydrated L-proline cadmium chloride for nonlinear optical applications, *Spectrochimica Acta Part A: Molecular and Biomolecular Spectroscopy*, (2015).
- [26] A. Irfan, A.G. Al-Sehemi, S. Muhammad, A.R. Chaudhry, M.S. Al-Assiri, R. Jin, A. Kalam, M. Shkir, A.M. Asiri, In-depth quantum chemical investigation of electro-optical and charge-transport properties of trans-3-(3,4-dimethoxyphenyl)-2-(4-nitrophenyl)prop-2-enenitrile, *Comptes Rendus Chimie*, 18 (2015) 1289-1296.
- [27] A. Irfan, A.G. Al-Sehemi, S. Muhammad, M.S. Al-Assiri, A.R. Chaudhry, A. Kalam, M. Shkir, Electro-optical and charge injection investigations of the donor- π -acceptor triphenylamine, oligocene-thiophene-pyrimidine and cyanoacetic acid based multifunctional dyes, *Journal of King Saud University - Science*, 27 (2015) 361-368.
- [28] A. Irfan, A.G. Al-Sehemi, DFT investigations of the ground and excited state geometries of the benzothiazine and benzisothiazol based anticancer drugs, *J. Saudi. Chem. Soc.*, 19 (2015) 318-321.
- [29] G. Keresztury, S. Holly, G. Besenyi, J. Varga, A. Wang, J. Durig, Vibrational spectra of monothiocarbamates-II. IR and Raman spectra, vibrational assignment, conformational analysis and ab initio calculations of S-methyl-N, N-dimethylthiocarbamate, *Spectrochimica Acta Part A: Molecular Spectroscopy*, 49 (1993) 2007-2026.

- [30] G. Keresztury, Raman spectroscopy: theory, Handbook of vibrational spectroscopy, (2002).
- [31] M. Govindarajan, M. Karabacak, Spectroscopic properties, NLO, HOMO–LUMO and NBO analysis of 2,5-Lutidine, Spectrochimica Acta Part A: Molecular and Biomolecular Spectroscopy, 96 (2012) 421-435.
- [32] P. Govindasamy, S. Gunasekaran, S. Srinivasan, Molecular geometry, conformational, vibrational spectroscopic, molecular orbital and Mulliken charge analysis of 2-acetoxybenzoic acid, Spectrochimica Acta Part A: Molecular and Biomolecular Spectroscopy, 130 (2014) 329-336.
- [33] S. Ramalingam, M. Karabacak, S. Periandy, N. Puviarasan, D. Tanuja, Spectroscopic (infrared, Raman, UV and NMR) analysis, Gaussian hybrid computational investigation (MEP maps/HOMO and LUMO) on cyclohexanone oxime, Spectrochimica Acta Part A: Molecular and Biomolecular Spectroscopy, 96 (2012) 207-220.
- [34] S. Ramalingam, S. Periandy, M. Govindarajan, S. Mohan, FTIR and FTRaman spectra, assignments, ab initio HF and DFT analysis of 4-nitrotoluene, Spectrochimica Acta Part A: Molecular and Biomolecular Spectroscopy, 75 (2010) 1308-1314.
- [35] T. Srikrishnan, R. Parthasarathy, Orientation And Intra-Molecular Hydrogen-Bonding Of Nitro-Groups In The Structure Of Picric Acid, In: Acta Crystallographica Section A, Munksgaard Int Publ Ltd 35 Norre Sogade, Po Box 2148, Dk-1016 Copenhagen, Denmark, 1978, Pp. S114-S114.
- [36] V. Ghazaryan, M. Fleck, A. Petrosyan, Structure and vibrational spectra of L-alanine L-alaninium picrate monohydrate, Journal of Molecular Structure, 1015 (2012) 51-55.

- [37] S. Guidara, H. Feki, Y. Abid, Vibrational spectral studies and non-linear optical properties of L-leucine L-leucinium picrate: a density functional theory approach, *Spectrochimica Acta Part A: Molecular and Biomolecular Spectroscopy*, 115 (2013) 437-444.
- [38] M.B. Mary, V. Sasirekha, V. Ramakrishnan, Vibrational spectral analysis of dl-valine dl-valinium and dl-methionine dl-methioninium picrates, *Spectrochimica Acta Part A: Molecular and Biomolecular Spectroscopy*, 65 (2006) 955-963.
- [39] G. Varsanyi, *Vibrational Spectra of Benzene Derivatives*, in, Academic Press, New York, 1969.
- [40] G. Varsanyi, *Assignments for Vibrational spectra of Seven Hundred Benzene Derivatives, I and II*, in, Adam Hilger, London,, 1974.
- [41] N. Sundaraganesan, S. Ilakiamani, H. Saleem, P.M. Wojciechowski, D. Michalska, FT-Raman and FT-IR spectra, vibrational assignments and density functional studies of 5-bromo-2-nitropyridine, *Spectrochimica Acta A*, 61 (2005) 2995-3001.
- [42] D.N. Sathyanarayana, *vibrational spectroscopy theory and application*, 2nd edition, , in, New Age International (P) Limited publishers, New Delhi, 2004.
- [43] J.H.S. Green, D.J. Harrison, W. Kynaston, *Vibrational spectra of benzene derivatives—XII 1,2,4-trisubstituted compounds*, *Spectrochimica Acta Part A: Molecular Spectroscopy*, 27 (1971) 807-815.
- [44] L.H.D.a.S.E.W. N.B. Clothup, *Introduction to Infrared and Raman spectroscopy*, in, Academic press Inc., London, 1964.
- [45] N.A.-D.J. Khaled Bahgat, Talaat El-Emary, *Theoretical and experimental investigations on the structure and vibrational spectra of 6-amino-3-methyl-1-phenyl-1H-pyrazolo-[3,4-b]pyridine-*

5-carboxylic acid and 6,7-dihydro-3-methyl-6-oxo-1-phenyl-1H-pyrazolo[3,4-b]pyridine-5-carbonitrile, *J. Serb. Chem. Soc.*, 74 (2009) 555-571.

[46] S. George, *Infrared and Raman characteristics group frequencies Tables and charts*, 3rd edition, in, Wiley, Chichester 2001.

[47] A. Pawlukojć, J. Leciejewicz, J. Tomkinson, S.F. Parker, Neutron scattering, infra red, Raman spectroscopy and ab initio study of l-threonine, *Spectrochimica Acta A*, 57 (2001) 2513-2523.

[48] K. Nakamoto, M. Margoshes, R.E. Rundle, Stretching Frequencies as a Function of Distances in Hydrogen Bonds, *J. Am. Chem. Soc.*, 77 (1955) 6480-6486.

[49] A. Vektariene, G. Vektaris, J. Svoboda, A theoretical approach to the nucleophilic behavior of benzofused thieno [3, 2-b] furans using DFT and HF based reactivity descriptors, *Arkivoc*, 7 (2009) 311-329.

[50] R.G. Pearson, Recent advances in the concept of hard and soft acids and bases, *Journal of Chemical Education*, 64 (1987) 561.

[51] C. Andraud, T. Brotin, C. Garcia, F. Pelle, P. Goldner, B. Bigot, A. Collet, Theoretical and experimental investigations of the nonlinear optical properties of vanillin, polyvanillin, and bisvanillin derivatives, *Journal of the American Chemical Society*, 116 (1994) 2094-2102.

[52] V.M. Geskin, C. Lambert, J.-L. Brédas, Origin of high second- and third-order nonlinear optical response in ammonio/borate diphenylpolyene zwitterions: the remarkable role of polarized aromatic groups, *Journal of the American Chemical Society*, 125 (2003) 15651-15658.

[53] D. Jacquemin, E.A. Perpète, G. Scalmani, M.J. Frisch, R. Kobayashi, C. Adamo, Assessment of the efficiency of long-range corrected functionals for some properties of large compounds, *The Journal of chemical physics*, 126 (2007) 144105.

- [54] M. de Wergifosse, B. Champagne, Electron correlation effects on the first hyperpolarizability of push–pull π -conjugated systems, *The Journal of Chemical Physics*, 134 (2011) 074113.
- [55] S. Muhammad, M. Shkir, S. AlFaify, A. Irfan, A.G. Al-Sehemi, Combined experimental and computational insights into the key features of l-alanine l-alaninium picrate monohydrate: growth, structural, electronic and nonlinear optical properties, *RSC Advances*, 5 (2015) 53988-54002.
- [56] K. Govindarasu, E. Kavitha, Vibrational spectra, molecular structure, NBO, UV, NMR, first order hyperpolarizability, analysis of 4-Methoxy-4'-Nitrobiphenyl by density functional theory, *Spectrochimica Acta Part A: Molecular and Biomolecular Spectroscopy*, 122 (2014) 130-141.
- [57] C. Adant, M. Dupuis, J. Bredas, Ab initio study of the nonlinear optical properties of urea: Electron correlation and dispersion effects, *International Journal of Quantum Chemistry*, 56 (1995) 497-507.
- [58] M. Karabacak, M. Cinar, FT-IR, FT-Raman, UV spectra and DFT calculations on monomeric and dimeric structure of 2-amino-5-bromobenzoic acid, *Spectrochimica Acta Part A: Molecular and Biomolecular Spectroscopy*, 86 (2012) 590-599.
- [59] R. Raju, C.Y. Panicker, P.S. Nayak, B. Narayana, B. Sarojini, C. Van Alsenoy, A.A. Al-Saadi, FT-IR, molecular structure, first order hyperpolarizability, MEP, HOMO and LUMO analysis and NBO analysis of 4-[(3-acetylphenyl) amino]-2-methylidene-4-oxobutanoic acid, *Spectrochimica Acta Part A: Molecular and Biomolecular Spectroscopy*, 134 (2015) 63-72.
- [60] R.N. Singh, A. Kumar, R.K. Tiwari, P. Rawat, V. Baboo, D. Verma, Molecular structure, heteronuclear resonance assisted hydrogen bond analysis, chemical reactivity and first hyperpolarizability of a novel ethyl-4-[[[(2,4-dinitrophenyl)-hydrazono]-ethyl]-3,5-dimethyl-1H-

pyrrole-2-carboxylate: A combined DFT and AIM approach, *Spectrochimica Acta Part A: Molecular and Biomolecular Spectroscopy*, 92 (2012) 295-304.

[61] K. Govindarasu, E. Kavitha, Molecular structure, vibrational spectra, NBO, UV and first order hyperpolarizability, analysis of 4-Chloro-dl-phenylalanine by density functional theory, *Spectrochimica Acta Part A: Molecular and Biomolecular Spectroscopy*, 133 (2014) 799-810.

[62] K. Govindarasu, E. Kavitha, N. Sundaraganesan, Synthesis, structural, spectral (FTIR, FT-Raman, UV, NMR), NBO and first order hyperpolarizability analysis of N-phenylbenzenesulfonamide by density functional theory, *Spectrochimica Acta Part A: Molecular and Biomolecular Spectroscopy*, 133 (2014) 417-431.

[63] G.A. Babu, P. Ramasamy, Crystal structure, crystal growth and characterization of novel organic NLO material: 2, 4, 4'-Trimethoxybenzophenone, *Materials Chemistry and Physics*, 119 (2010) 533-538.

Supporting information

Molecular structure, vibrational, photophysical and nonlinear optical properties of L-threoninium picrate: A first-principles study

S. AlFaify^{a}, Mohd. Shkir^{a*}, Manju Arora^b, Ahmad Irfan^{c,d}, H. Algarni^a, Haider Abbas^e, Abdullah G. Al-Sehemi^{c,d}*

^aDepartment of Physics, Faculty of Science, King Khalid University, P.O. Box. 9004 Abha 61413, Saudi Arabia

^bCSIR- National Physical Laboratory, Dr. K.S. Krishnan Road, New Delhi 110012, India

^cDepartment of Chemistry, Faculty of Science, King Khalid University, Abha 61413, P.O. Box 9004, Saudi Arabia

^dResearch Center for Advanced Materials Science, King Khalid University, Abha 61413, P.O. Box 9004, Saudi Arabia

^eDepartment of Physics, Manav Rachna College of Engineering, Faridabad, Haryana 121001, India

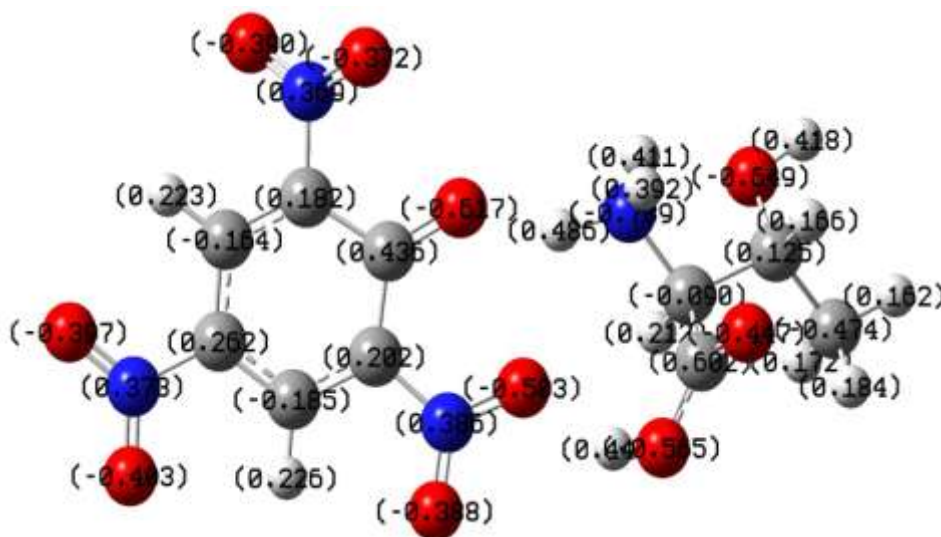


Fig. S1. Mulliken charges of LTHP molecule

Table S1 Mulliken charge analysis of L-threonine picrate (LTHP) molecule.

Atom No.	Atom	Mulliken charge
1	C	0.60181
2	C	-0.09022
3	H	0.21167
4	C	0.12460
5	H	0.16569
6	C	-0.47418
7	H	0.17241
8	H	0.18383
9	H	0.16228
10	N	-0.78857
11	H	0.48554
12	H	0.41110
13	H	0.39242
14	O	-0.44743
15	O	-0.56457
16	O	-0.64856
17	H	0.41760
18	C	0.43593
19	C	0.18196
20	C	-0.16405
21	H	0.22276
22	C	0.26184
23	C	-0.18510
24	H	0.22591
25	C	0.20222
26	N	0.36907
27	N	0.37302
28	N	0.38573
29	O	-0.61733
30	O	-0.37246
31	O	-0.38985
32	O	-0.39731
33	O	-0.40261
34	O	-0.38779
35	O	-0.50334
36	H	0.44600

Table S2 Calculated IR and Raman frequencies with their assignments of LTHP obtained by DFT using B3LYP/6-31G* and HF/6-31G* levels of theory.

Reported [22]		Current work			
		B3LYP		HF	
IR frequencies (cm ⁻¹)	Assignments	IR frequencies (cm ⁻¹)	Raman Frequencies (cm ⁻¹)	IR frequencies (cm ⁻¹)	Raman Frequencies (cm ⁻¹)
3400	O-H stretching	3340	3334	3348	3348
3238	N-H, NH ₂ symmetric stretching	3271, 3150	3265,3135	3276	3277
2914	C-H stretching	3037,3011,2920	3031,2945,2884	3089,2837	3090,2980
1745	C=O Asymmetric stretching	1780	1777	1810	1812
1612	NH ₃ ⁺ Asymmetric deformation, C=C ring vibration	1633	1630	1678,1642	1770
1570	NO ₂ Asymmetric stretching	1607	1605	1578	1580
1541	NH ₃ symmetric stretching	1546	1561,1543	1535	1540,1535
1493	CH ₃ Asymmetric deformation	1492	1509,1465	1465	1509,1465
1425	NO ₂ stretching	1416,1398	1414	1437,1400	1437
----	NO ₂ symmetric stretching	1347,1330,1312	1344,1327	1338	1339
1273	CH ₃ deformation, C-O phenolic, symmetric (C-OH) stretching	1278	1310, 1275	1223	1225
1163	C=O stretching	1165,1140	1170,1137	1190,1151	1160
1098	C=C stretching	1096,1061	1093	1080	1080
918	C-C stretching/ring	905	929,903,860	930	946
787	C-C skeletal stretching	818	834,799,765	792	805
743	NO ₂ scissoring	766	747,721,707	741,714	723
706	NO ₂ bending, C-H bending, COO ⁻ deformation	705,698	678,661,644	696	698
542	C-C-N deformation, ρ(NO ₂)	532	532	553	535
—	Skeletal deformation/lattice vibrations	385,263,203	427,367,323,263, 194,150,55,12	450, 366,267, 196	450,366,321, 196

NLO properties methodology

For calculating the above said parameters the mathematical expressions are defined as:

Dipole moment

$$\mu_{tot} = (\mu_x^2 + \mu_y^2 + \mu_z^2)^{\frac{1}{2}} \quad (3)$$

Total average polarizability

$$\alpha_0 = \frac{1}{3}(\alpha_{xx} + \alpha_{yy} + \alpha_{zz}) \quad (4)$$

Anisotropy of polarizability

$$\Delta\alpha = \frac{1}{\sqrt{2}} \sqrt{[(\alpha_{xx} - \alpha_{yy})^2 + (\alpha_{yy} - \alpha_{zz})^2 + (\alpha_{zz} - \alpha_{xx})^2 + 6\alpha_{xz}^2]} \quad (5)$$

Components of first hyperpolarizability can be calculated by using the expression

$$\beta_i = \beta_{iii} + \sum_{i \neq j} \left[\frac{(\beta_{ijj} + 2\beta_{jii})}{3} \right] \quad (6)$$

Using x, y, z components the magnitude of first hyperpolarizability (β_{tot}) can be calculated as:

$$\beta_{tot} = \sqrt{(\beta_x^2 + \beta_y^2 + \beta_z^2)} \quad (7)$$

Where β_x , β_y and β_z are:

$$\beta_x = (\beta_{xxx} + \beta_{xxy} + \beta_{xyy})$$

$$\beta_y = (\beta_{yyy} + \beta_{xxz} + \beta_{yyz})$$

$$\beta_z = (\beta_{xzz} + \beta_{yzz} + \beta_{zzz})$$

Hence, the final equation for magnitude of total first static hyperpolarizability calculation is given by

$$\beta_{tot} = \sqrt{[(\beta_{xxx} + \beta_{xxy} + \beta_{xyy})^2 + (\beta_{yyy} + \beta_{xxz} + \beta_{yyz})^2 + (\beta_{xzz} + \beta_{yzz} + \beta_{zzz})^2]} \quad (8)$$

The first hyperpolarizability can be described by a $3 \times 3 \times 3$ matrix as it is known as a third order tensor and 27 components of the 3D matrix are reduced to 10 components due to the Kleinman symmetry [64], and can be given in lower tetrahedral format. It is obvious that the lower part of $3 \times 3 \times 3$ matrices is tetrahedral. The static first hyperpolarizability was also calculated using the following relation, $\beta_0 = \frac{3}{5}\beta_{tot}$. The calculated values of 6 components of polarizability, 3 components of dipole moment and 10 components of hyperpolarizability along with their total values with or without conversion i.e. a.u. and esu., are presented in Table 2, as for α , 1 a.u.= 0.1482×10^{-24} esu and for β , 1 a.u.= 0.008639×10^{-30} . The electronic communication of two different parts of any compound plays a vital role in polarizability and hyperpolarizability values. The variation of total dipole moment and first hyperpolarizability values calculated by B3LYP, CAM-B3LYP and LC-BLYP functional in comparison of reported value of urea are shown in Fig. S2 (a) and (b).

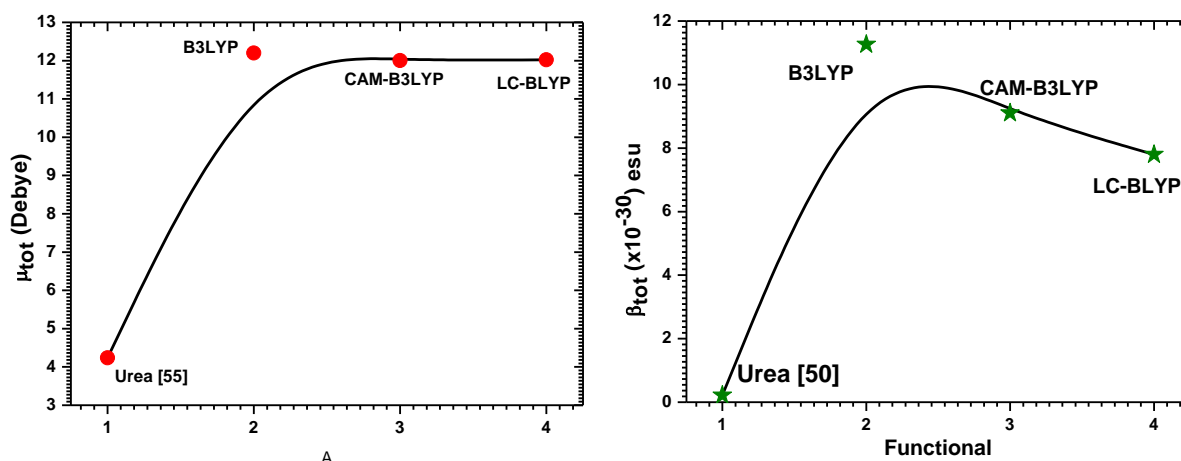


Fig. S2. Variation of (a) dipole moment and (b) first hyperpolarizability calculated by different functionals at 6-31G* basis set.

Global chemical reactivity descriptors

An approximation for absolute hardness η was developed [65-67] as given below:

$$\eta = \frac{I - A}{2} \quad (8)$$

where I is the vertical ionization energy and A is vertical electron affinity.

As per Koopmans theorem [68] the ionization energy and electron affinity can be specified through HOMO and LUMO orbital energies as:

$$I = -E_{\text{HOMO}}$$

$$A = -E_{\text{LUMO}}$$

Values of I and A of LTHP molecules calculated at both level of theories are given in Table S3.

The higher energy of HOMO is corresponds to the more reactive molecule in the reactions with electrophiles, while lower LUMO energy is essential for molecular reactions with nucleophiles [69].

Hence, the hardness of any materials is corresponds to the gap between the HOMO and LUMO orbitals. If the energy gap of HOMO-LUMO is larger then molecule would be harder [66].

$$\eta = \frac{1}{2} (E_{\text{LUMO}} - E_{\text{HOMO}}) \quad (9)$$

The electronic chemical potential of a molecule is calculated by:

$$\mu = -\left(\frac{I + A}{2}\right) \quad (10)$$

The softness of a molecule is calculated by:

$$S = \frac{1}{2\eta} \quad (11)$$

The electronegativity of the molecule is calculated by:

$$\chi = \left(\frac{I + A}{2}\right) \quad (12)$$

The electrophilicity index of the molecule is calculated by:

$$\omega = \frac{\mu^2}{2\eta} \quad (13)$$

The calculated values of GCRD such as η , μ , S , χ and ω for LTHP molecule are also presented in Table S3.

Table S3

Calculated energy values of FMOs, their difference, η , μ , S , χ and ω at B3LYP/6-31G* basis set for LTHP molecule in G.S.

<i>Parameters</i>	<i>B3LYP (e.V.)</i>
E_{HOMO}	-6.674
E_{HOMO-1}	-7.345
E_{LUMO}	-3.114
E_{LUMO+1}	-2.226
$\Delta E_{HOMO-LUMO}$	3.559
$\Delta E_{HOMO-1-LUMO+1}$	5.119
<i>Hardness (η)</i>	1.780
<i>Potential (μ)</i>	-4.894
<i>Softness (S)</i>	1.875
<i>Electronegativity (χ)</i>	4.894
<i>Electrophilic index (ω)</i>	6.728

References

- [1] B. Saleh, MC Teich Fundamentals of photonics, in, New York: John Wiley & Sons, 1991.
- [2] B.G. Penn, B.H. Cardelino, C.E. Moore, A.W. Shields, D. Frazier, Growth of bulk single crystals of organic materials for nonlinear optical devices: An overview, Progress in Crystal Growth and Characterization of Materials, 22 (1991) 19-51.
- [3] M. Shakir, B. Singh, B. Kumar, G. Bhagavannarayana, Ferroelectricity in glycine picrate: An astonishing observation in a centrosymmetric crystal, Applied Physics Letters, 95 (2009) 252902-252902-252903.
- [4] Mohd. Shakir, G. Bhagavannarayana, B. K. Singh, Binay Kumar, Organic ferroelectrics: A big surprise, NPG Asia Materials, (2010).

- [5] M. Ravi, P. Gangopadhyay, D.N. Rao, S. Cohen, I. Agranat, T.P. Radhakrishnan, Dual Influence of H-Bonding on the Solid-State Second- Harmonic Generation of a Chiral Quinonoid Compound, *Chemistry of Materials*, 10 (1998) 2371-2377.
- [6] P. Franken, J. Ward, Optical harmonics and nonlinear phenomena, *Reviews of Modern Physics*, 35 (1963) 23.
- [7] J.M. Cole, C.C. Wilson, J.A. Howard, F.R. Cruickshank, Quantitative analysis of hydrogen bonding and atomic thermal motion in the organic non-linear optical material DCNP using X-ray and neutron diffraction, *Acta Crystallographica Section B: Structural Science*, 56 (2000) 1085-1093.
- [8] J. Zyss, J. Nicoud, M. Coquillay, Chirality and hydrogen bonding in molecular crystals for phase-matched second-harmonic generation: N-(4-nitrophenyl)-(L)-prolinol (NPP), *The Journal of chemical physics*, 81 (1984) 4160-4167.
- [9] I. Ledoux, J. Badan, J. Zyss, A. Migus, D. Hulin, J. Etchepare, G. Grillon, A. Antonetti, Generation of high-peak-power tunable infrared femtosecond pulses in an organic crystal: application to time resolution of weak infrared signals, *JOSA B*, 4 (1987) 987-997.
- [10] A. Datta, S.K. Pati, Dipole orientation effects on nonlinear optical properties of organic molecular aggregates, *The Journal of chemical physics*, 118 (2003) 8420-8427.
- [11] M. Shakir, S. Kushwaha, K. Maurya, M. Arora, G. Bhagavannarayana, Growth and characterization of glycine picrate—Remarkable second-harmonic generation in centrosymmetric crystal, *Journal of crystal growth*, 311 (2009) 3871-3875.
- [12] T. KAI, M. GoTo, K. FURUHATA, H. TAKAYANAGI, Crystal structure of glycine picrate, *Analytical Sciences*, 10 (1994) 359-360.

- [13] P. Srinivasan, T. Kanagasekaran, R. Gopalakrishnan, G. Bhagavannarayana, P. Ramasamy, Studies on the Growth and Characterization of l-Asparaginium Picrate (LASP) A Novel Nonlinear Optical Crystal, *Crystal growth & design*, 6 (2006) 1663-1670.
- [14] M. Shkir, B. Riscob, G. Bhagavannarayana, Synthesis, growth, structural, spectroscopic, crystalline perfection, second harmonic generation (SHG) and thermal studies of 2-aminopyridinium picrate (2APP): A new nonlinear optical material, *Solid State Sciences*, 14 (2012) 773-776.
- [15] A. Aarthy, K. Anitha, S. Athimoolam, S.A. Bahadur, R. Rajaram, L-Asparaginium nitrate, *Acta Crystallographica Section E: Structure Reports Online*, 61 (2005) 2042-2044.
- [16] S. Natarajan, M. Umamaheswaran, J. Kalyana Sundar, J. Suresh, S.A. Martin Britto Dhas, Structural, spectroscopic and nonlinear optical studies on a new efficient organic donor–acceptor crystal for second harmonic generation: l-Threoninium picrate, *Spectrochimica Acta Part A: Molecular and Biomolecular Spectroscopy*, 77 (2010) 160-163.
- [17] A. Irfan, A.G. Al-Sehemi, A. Rasool Chaudhry, S. Muhammad, The structural, electro-optical, charge transport and nonlinear optical properties of oxazole (4Z)-4-Benzylidene-2-(4-methylphenyl)-1,3-oxazol-5(4H)-one derivative, *Journal of King Saud University - Science*, <http://dx.doi.org/10.1016/j.jksus.2016.10.004> (2016).
- [18] A. Irfan, A.G. Al-Sehemi, A.R. Chaudhry, S. Muhammad, A.M. Asiri, The structural, electro-optical, charge transport and nonlinear optical properties of 2-[(3,5-dimethyl-1-phenyl-1H-pyrazol-4-yl)methylidene]indan-1,3-dione, *Optik*, 127 (2016) 10148-10157.
- [19] M. Shkir, H. Abbas, Physico chemical properties of l-asparagine l-tartaric acid single crystals: A new nonlinear optical material, *Spectrochimica Acta Part A: Molecular and Biomolecular Spectroscopy*, 118 (2014) 172-176.

- [20] M.E. Foster, B.M. Wong, Nonempirically tuned range-separated DFT accurately predicts both fundamental and excitation gaps in DNA and RNA nucleobases, *Journal of chemical theory and computation*, 8 (2012) 2682-2687.
- [21] B.M. Wong, M. Piacenza, F. Della Sala, Absorption and fluorescence properties of oligothiophene biomarkers from long-range-corrected time-dependent density functional theory, *Physical Chemistry Chemical Physics*, 11 (2009) 4498-4508.
- [22] G.V. Gibbs, T.D. Crawford, A.F. Wallace, D.F. Cox, R.M. Parrish, E.G. Hohenstein, C.D. Sherrill, Role of Long-Range Intermolecular Forces in the Formation of Inorganic Nanoparticle Clusters, *The Journal of Physical Chemistry A*, 115 (2011) 12933-12940.
- [23] M. Shkir, S. AlFaify, H. Abbas, G. Bhagavannarayana, A physico-chemical approach to study the experimental and theoretical properties of l-ornithine monohydrochloride: An organic nonlinear optical material, *Materials Chemistry and Physics*, (2015).
- [24] M. Shkir, S. AlFaify, H. Abbas, S. Muhammad, First principal studies of spectroscopic (IR and Raman, UV-visible), molecular structure, linear and nonlinear optical properties of L-arginine p-nitrobenzoate monohydrate (LANB): a new non-centrosymmetric material, *Spectrochimica Acta Part A: Molecular and Biomolecular Spectroscopy*, (2015).
- [25] M. Shkir, S. Muhammad, S. AlFaify, Experimental and density functional theory (DFT): a dual approach to study the various important properties of monohydrated L-proline cadmium chloride for nonlinear optical applications, *Spectrochimica Acta Part A: Molecular and Biomolecular Spectroscopy*, (2015).
- [26] A. Irfan, A.G. Al-Sehemi, S. Muhammad, A.R. Chaudhry, M.S. Al-Assiri, R. Jin, A. Kalam, M. Shkir, A.M. Asiri, In-depth quantum chemical investigation of electro-optical and charge-

transport properties of trans-3-(3,4-dimethoxyphenyl)-2-(4-nitrophenyl)prop-2-enenitrile, *Comptes Rendus Chimie*, 18 (2015) 1289-1296.

[27] A. Irfan, A.G. Al-Sehemi, S. Muhammad, M.S. Al-Assiri, A.R. Chaudhry, A. Kalam, M. Shkir, Electro-optical and charge injection investigations of the donor- π -acceptor triphenylamine, oligocene-thiophene-pyrimidine and cyanoacetic acid based multifunctional dyes, *Journal of King Saud University - Science*, 27 (2015) 361-368.

[28] A. Irfan, A.G. Al-Sehemi, DFT investigations of the ground and excited state geometries of the benzothiazine and benzisothiazol based anticancer drugs, *J. Saudi. Chem. Soc.*, 19 (2015) 318-321.

[29] G. Keresztury, S. Holly, G. Besenyi, J. Varga, A. Wang, J. Durig, Vibrational spectra of monothiocarbamates-II. IR and Raman spectra, vibrational assignment, conformational analysis and ab initio calculations of S-methyl-N, N-dimethylthiocarbamate, *Spectrochimica Acta Part A: Molecular Spectroscopy*, 49 (1993) 2007-2026.

[30] G. Keresztury, Raman spectroscopy: theory, *Handbook of vibrational spectroscopy*, (2002).

[31] M. Govindarajan, M. Karabacak, Spectroscopic properties, NLO, HOMO-LUMO and NBO analysis of 2,5-Lutidine, *Spectrochimica Acta Part A: Molecular and Biomolecular Spectroscopy*, 96 (2012) 421-435.

[32] P. Govindasamy, S. Gunasekaran, S. Srinivasan, Molecular geometry, conformational, vibrational spectroscopic, molecular orbital and Mulliken charge analysis of 2-acetoxybenzoic acid, *Spectrochimica Acta Part A: Molecular and Biomolecular Spectroscopy*, 130 (2014) 329-336.

[33] S. Ramalingam, M. Karabacak, S. Periandy, N. Puviarasan, D. Tanuja, Spectroscopic (infrared, Raman, UV and NMR) analysis, Gaussian hybrid computational investigation (MEP

maps/HOMO and LUMO) on cyclohexanone oxime, *Spectrochimica Acta Part A: Molecular and Biomolecular Spectroscopy*, 96 (2012) 207-220.

[34] S. Ramalingam, S. Periandy, M. Govindarajan, S. Mohan, FTIR and FTRaman spectra, assignments, ab initio HF and DFT analysis of 4-nitrotoluene, *Spectrochimica Acta Part A: Molecular and Biomolecular Spectroscopy*, 75 (2010) 1308-1314.

[35] T. SRIKRISHNAN, R. PARTHASARATHY, ORIENTATION AND INTRA-MOLECULAR HYDROGEN-BONDING OF NITRO-GROUPS IN THE STRUCTURE OF PICRIC ACID, in: *ACTA CRYSTALLOGRAPHICA SECTION A*, MUNKSGAARD INT PUBL LTD 35 NORRE SOGADE, PO BOX 2148, DK-1016 COPENHAGEN, DENMARK, 1978, pp. S114-S114.

[36] V. Ghazaryan, M. Fleck, A. Petrosyan, Structure and vibrational spectra of L-alanine L-alaninium picrate monohydrate, *Journal of Molecular Structure*, 1015 (2012) 51-55.

[37] S. Guidara, H. Feki, Y. Abid, Vibrational spectral studies and non-linear optical properties of L-leucine L-leucinium picrate: a density functional theory approach, *Spectrochimica Acta Part A: Molecular and Biomolecular Spectroscopy*, 115 (2013) 437-444.

[38] M.B. Mary, V. Sasirekha, V. Ramakrishnan, Vibrational spectral analysis of dl-valine dl-valinium and dl-methionine dl-methioninium picrates, *Spectrochimica Acta Part A: Molecular and Biomolecular Spectroscopy*, 65 (2006) 955-963.

[39] G. Varsanyi, *Vibrational Spectra of Benzene Derivatives*, in, Academic Press, New York, 1969.

[40] G. Varsanyi, *Assignments for Vibrational spectra of Seven Hundred Benzene Derivatives*, I and II, in, Adam Hilger, London,, 1974.

- [41] N. Sundaraganesan, S. Ilakiamani, H. Saleem, P.M. Wojciechowski, D. Michalska, FT-Raman and FT-IR spectra, vibrational assignments and density functional studies of 5-bromo-2-nitropyridine, *Spectrochimica Acta A*, 61 (2005) 2995-3001.
- [42] D.N. Sathyanarayana, vibrational spectroscopy theory and application, 2nd edition, , in, New Age International (P) Limited publishers, New Delhi, 2004.
- [43] J.H.S. Green, D.J. Harrison, W. Kynaston, Vibrational spectra of benzene derivatives—XII 1,2,4-trisubstituted compounds1, *Spectrochimica Acta Part A: Molecular Spectroscopy*, 27 (1971) 807-815.
- [44] L.H.D.a.S.E.W. N.B. Clothup, Introduction to Infrared and Raman spectroscopy, in, Academic press Inc., London, 1964.
- [45] N.A.-D.J. KHALED BAHGAT, TALAAT EL-EMARY, Theoretical and experimental investigations on the structure and vibrational spectra of 6-amino-3-methyl-1-phenyl-1H-pyrazolo-[3,4-b]pyridine-5-carboxylic acid and 6,7-dihydro-3-methyl-6-oxo-1-phenyl-1H-pyrazolo[3,4-b]pyridine-5-carbonitrile, *J. Serb. Chem. Soc.*, 74 (2009) 555-571.
- [46] S.George, Infrared and Raman characteristics group frequencies Tables and charts, 3rd edition, in, wiley, chichester 2001.
- [47] A. Pawlukoć, J. Leciejewicz, J. Tomkinson, S.F. Parker, Neutron scattering, infra red, Raman spectroscopy and ab initio study of l-threonine, *Spectrochimica Acta A*, 57 (2001) 2513-2523.
- [48] K. Nakamoto, M. Margoshes, R.E. Rundle, Stretching Frequencies as a Function of Distances in Hydrogen Bonds, *J. Am. Chem. Soc.*, 77 (1955) 6480-6486.

- [49] A. Vektariene, G. Vektaris, J. Svoboda, A theoretical approach to the nucleophilic behavior of benzofused thieno [3, 2-b] furans using DFT and HF based reactivity descriptors, *Arkivoc*, 7 (2009) 311-329.
- [50] R.G. Pearson, Recent advances in the concept of hard and soft acids and bases, *Journal of Chemical Education*, 64 (1987) 561.
- [51] C. Andraud, T. Brotin, C. Garcia, F. Pelle, P. Goldner, B. Bigot, A. Collet, Theoretical and experimental investigations of the nonlinear optical properties of vanillin, polyvanillin, and bisvanillin derivatives, *Journal of the American Chemical Society*, 116 (1994) 2094-2102.
- [52] V.M. Geskin, C. Lambert, J.-L. Brédas, Origin of high second- and third-order nonlinear optical response in ammonio/borate diphenylpolyene zwitterions: the remarkable role of polarized aromatic groups, *Journal of the American Chemical Society*, 125 (2003) 15651-15658.
- [53] D. Jacquemin, E.A. Perpète, G. Scalmani, M.J. Frisch, R. Kobayashi, C. Adamo, Assessment of the efficiency of long-range corrected functionals for some properties of large compounds, *The Journal of chemical physics*, 126 (2007) 144105.
- [54] M. de Wergifosse, B. Champagne, Electron correlation effects on the first hyperpolarizability of push-pull π -conjugated systems, *The Journal of Chemical Physics*, 134 (2011) 074113.
- [55] S. Muhammad, M. Shkir, S. AlFaify, A. Irfan, A.G. Al-Sehemi, Combined experimental and computational insights into the key features of l-alanine l-alaninium picrate monohydrate: growth, structural, electronic and nonlinear optical properties, *RSC Advances*, 5 (2015) 53988-54002.

- [56] K. Govindarasu, E. Kavitha, Vibrational spectra, molecular structure, NBO, UV, NMR, first order hyperpolarizability, analysis of 4-Methoxy-4'-Nitrobiphenyl by density functional theory, *Spectrochimica Acta Part A: Molecular and Biomolecular Spectroscopy*, 122 (2014) 130-141.
- [57] C. Adant, M. Dupuis, J. Bredas, Ab initio study of the nonlinear optical properties of urea: Electron correlation and dispersion effects, *International Journal of Quantum Chemistry*, 56 (1995) 497-507.
- [58] M. Karabacak, M. Cinar, FT-IR, FT-Raman, UV spectra and DFT calculations on monomeric and dimeric structure of 2-amino-5-bromobenzoic acid, *Spectrochimica Acta Part A: Molecular and Biomolecular Spectroscopy*, 86 (2012) 590-599.
- [59] R. Raju, C.Y. Panicker, P.S. Nayak, B. Narayana, B. Sarojini, C. Van Alsenoy, A.A. Al-Saadi, FT-IR, molecular structure, first order hyperpolarizability, MEP, HOMO and LUMO analysis and NBO analysis of 4-[(3-acetylphenyl) amino]-2-methylidene-4-oxobutanoic acid, *Spectrochimica Acta Part A: Molecular and Biomolecular Spectroscopy*, 134 (2015) 63-72.
- [60] R.N. Singh, A. Kumar, R.K. Tiwari, P. Rawat, V. Baboo, D. Verma, Molecular structure, heteronuclear resonance assisted hydrogen bond analysis, chemical reactivity and first hyperpolarizability of a novel ethyl-4-[(2,4-dinitrophenyl)-hydrazono]-ethyl}-3,5-dimethyl-1H-pyrrole-2-carboxylate: A combined DFT and AIM approach, *Spectrochimica Acta Part A: Molecular and Biomolecular Spectroscopy*, 92 (2012) 295-304.
- [61] K. Govindarasu, E. Kavitha, Molecular structure, vibrational spectra, NBO, UV and first order hyperpolarizability, analysis of 4-Chloro-dl-phenylalanine by density functional theory, *Spectrochimica Acta Part A: Molecular and Biomolecular Spectroscopy*, 133 (2014) 799-810.
- [62] K. Govindarasu, E. Kavitha, N. Sundaraganesan, Synthesis, structural, spectral (FTIR, FT-Raman, UV, NMR), NBO and first order hyperpolarizability analysis of N-

phenylbenzenesulfonamide by density functional theory, *Spectrochimica Acta Part A: Molecular and Biomolecular Spectroscopy*, 133 (2014) 417-431.

[63] G.A. Babu, P. Ramasamy, Crystal structure, crystal growth and characterization of novel organic NLO material: 2, 4, 4'-Trimethoxybenzophenone, *Materials Chemistry and Physics*, 119 (2010) 533-538.

[64] D. Kleinman, Nonlinear dielectric polarization in optical media, *Physical Review*, 126 (1962) 1977.

[65] R.G. Parr, P.K. Chattaraj, Principle of maximum hardness, *Journal of the American Chemical Society*, 113 (1991) 1854-1855.

[66] R.G. Pearson, Absolute electronegativity and absolute hardness of Lewis acids and bases, *Journal of the American Chemical Society*, 107 (1985) 6801-6806.

[67] R.G. Parr, R.G. Pearson, Absolute hardness: companion parameter to absolute electronegativity, *Journal of the American Chemical Society*, 105 (1983) 7512-7516.

[68] T. Koopmans, Ordering of wave functions and eigenenergies to the individual electrons of an atom, *Physica*, 1 (1933) 104-113.

[69] A. Rauk, *Orbital interaction Theory of Organic Chemistry*, 2nd Edn John Wiley & Sons: Newyork, 2001, 34 (2001).